Plasma Phys. Control. Fusion **39** (1997) 1841–1859. Printed in the UK PII: S0741-3335(97)80488-5

Low-aspect-ratio stellarators with planar coils

Paul E Moroz

Center for Plasma Theory and Computation, Department of Engineering Physics, University of Wisconsin, Madison, WI 53706, USA

Received 30 December 1996, in final form 8 August 1997

Abstract. The possibility of using simple sets of planar coils to produce low-aspect-ratio stellarator (LARS) configurations is analysed. Various types of LARS with different planar coils of potential interest to fusion research are identified. It is found that these configurations possess rather attractive features including: compact design and coil simplicity; good access to the plasma; closed vacuum flux surfaces with large enclosed volume; a significant external rotational transform; strong magnetic well; and a natural divertor. Finite plasma-pressure and finite plasma-current effects are studied as well, and it is shown that the LARS configurations considered benefit from the plasma current.

1. Introduction

In spite of the significant progress in fusion research which has led to regimes generating noticeable amounts of fusion energy [1], there are still a few serious problems to overcome before achieving an inexpensive, efficient and safe thermonuclear reactor.

Strong plasma current, which plays a key role in good plasma confinement and efficient plasma heating in tokamaks also involves some negative and dangerous effects. One of the main effects is the possibility of a major disruption which might cause serious damage to various reactor components. It is also an issue of safety. All measures have to be taken to guarantee the absence of disruptions in the reactor environment. Another problem is that a significant portion of the plasma current has to be externally driven (via rf waves or neutral-beam injection), which is expensive and leads to an increase in the cost of electricity production. Both of these problems can be partially solved if a tokamak is capable of working efficiently with reduced plasma current. A tokamak–stellarator hybrid might be advantageous from this point of view because the part of the rotational transform, normally generated by the plasma current, can be produced by external coils.

Stellarators do not have the two above-mentioned problems. However, they have a few other drawbacks. Because of the three-dimensional character of the magnetic field in stellarators, it is more difficult to reach good plasma confinement in the collisionless (banana) regime of the hot thermonuclear plasma. Also, because of the absence of ohmic heating, a much more powerful auxiliary heating system is required for a stellarator reactor to reach ignition. The complications of the coil system and the strict requirements on the accuracy of the coil manufacturing and assembly process represent another set of drawbacks.

Both systems, tokamaks and stellarators, can lead, in principle, to the construction of a fusion reactor. One of the most important current international projects of this type is ITER (International Thermonuclear Experimental Reactor) [2]. In parallel to further developing

0741-3335/97/111841+19$19.50

the main established fusion concepts, such as tokamaks, stellarators, reversed-field pinches and spheromaks, it is also important to search for a more efficient approach to controlled fusion by considering significantly different configurations and hybrids between different concepts.

In this paper we present an analysis of various simple low-aspect-ratio stellarator (LARS) configurations, with $A \leqslant 3.5$ (the aspect ratio A is the ratio of the average major radius R to the average minor radius ρ for the last closed flux surface). These configurations are unique in comparison with the presently existing large-aspect-ratio stellarators for which $A \approx 5$–11. This analysis is a continuation of our previous research [3–6] on a novel concept for magnetic fusion called the Spherical Stellarator (SS), which was originally proposed in [3].

It should be noted that the lowest-aspect-ratio stellarators ever built, the Compact Helical System (CHS) [7], the Compact Auburn Torsatron (CAT) [8], and heliac H-1 [9], have $A \approx 5$. In the SS concept, the plasma aspect ratio is much lower, usually about, or sometimes significantly below $A = 3.5$; also, the use of modular coils in a SS represents a significant advantage for reactor applications where the possibility of replacing any particular part of a device has to be maintained. In [4–6], it was shown that combining the plasma current and the external stellarator rotational transform in a SS produces strongly positive effects, such as the possibility of high-β equilibria (β is the ratio of the thermal plasma energy to the magnetic-field energy) and the decreased magnetic-field ripple. It was also shown that at high β a relatively strong bootstrap current exists in a SS, which might be enough to obtain these advantageous characteristics. However, for the first relatively small SS devices, it is reasonable to use an ohmic current transformer for magnetic configuration improvement and for plasma heating, thus the first SS device will probably be a stellarator–tokamak hybrid. Further discussion of the advantages of the SS concept and projections for large plasmas are given in [6].

In this paper we make a further step in simplifying the coil configuration of a LARS. In particular, we only limit ourselves to the consideration of the planar coils. Moreover, all coils are the same and carry the same current, so the system looks like a toroidally symmetric one, similar to a tokamak, but has stellarator features. Such a system can benefit from the plasma current, similar to the above-mentioned SS configurations [3–6]. We consider the simplicity of the coils as a very important factor. This means not only that the corresponding device will be inexpensive to construct (which is very important in itself), but also that the coil-system manufacturing and spatial assembly can be done much more precisely than for a typical stellarator. Hence, the magnetic-field disturbances due to the inaccuracy of manufacturing or assembly, causing the appearance of magnetic islands and poor plasma confinement, might be much lower.

Historically the use of planar coils for the production of stellarator effects has been considered in a number of publications [10–15]. A more recent and detailed analysis of this type of configuration has been given in [16]. That paper was devoted to the analysis and optimization of stellarator characteristics of configurations with planar inclined coils. The present paper can be viewed as a continuation of that work. Here we use the same rules and methods for the configuration optimization as those formulated in [16]. This time, however, we concentrate on reducing the aspect-ratio parameter A and consider more complicated, although planar, coils. The LARS (or tokamak–stellarator hybrid) devices represent a novel area of research with substantially different physics in comparison with that for large-A devices and require separate consideration. This is somewhat similar to the well known Spherical Tokamak approach (see, e.g., [17]) which is facing a lot of new physics in comparison with that for standard tokamaks.

The paper is organized as follows. In section 2 a LARS configuration with planar circular coils is considered. In section 3 the LARS configurations with planar coils capable of producing bean-shaped vacuum flux surfaces are discussed. An example of the planar coil system capable of accommodating the central ohmic current transformer without increasing the size of a system is considered in section 4. The configuration of a natural divertor in the LARS with planar coils is analysed in section 5. Finite β and finite plasma-current effects are considered in section 6. The application of global stellarator scalings to LARS is discussed in section 7. Finally the main conclusions are given in section 8.

2. Low-aspect-ratio stellarator with circular coils

Planar circular coils are very convenient and inexpensive to manufacture. Many fusion experiments, including tokamaks, were first designed and operated with circular coils. Only later was it shown that tokamaks with D-shaped elongated plasma, and hence D-shaped coils, have definite advantages in obtaining better plasma parameters. Even stellarators, such as the presently operational heliacs, TJ-II [18] or H-1 [9], make use of the circular coils.

In this section we consider the same device with planar circular inclined coils as reported in [16]. This time, however, the aspect ratio A is much lower; also, the number of the inclined toroidal field (TF) coils was chosen to be six instead of nine as it was in [16]. It is reasonable to decrease the number of TF coils for a LARS machine as there is not much space in the centre of the device for many coils. On the other hand, devices with N TF coils (with N lower than four), in spite of the fact that very low-A magnetic-field configurations can be produced there, are probably too open for the magnetic-field disturbances and correspond to too high magnetic-field ripple. Six TF coils probably corresponds to a reasonable compromise between the lowest aspect ratio and the advanced characteristics of the magnetic-field structure, although in general the values of N between four and twelve are of interest for a LARS device with planar coils.

By using the three optimization rules discussed in [16], we were able to obtain a number of configurations with promising parameters. We will present just one particular case. The coil system of a stellarator considered with six planar circular inclined TF coils and six poloidal-field (PF) rings, as well as the last closed vacuum flux surface, are shown in figure 1(a) (side view) and figure 1(b) (top view). The plasma aspect ratio $A \approx 2.4$. The set of closed flux surfaces obtained is presented in figure 2, where three main cross sections are shown: (a) under the TF coil, $\varphi = 0$, (b) at $1/4$ of the field period, $\varphi = \pi/2N$, and (c) at $1/2$ of the field period, i.e. between the TF coils, $\varphi = \pi/N$, φ being the toroidal angle. For a better presentation of the closed flux surfaces figure 2 differs slightly from the usually calculated puncture plots in that the neighbouring points are connected by straight lines (for comparison, the puncture plots for the similar but larger A device are given in [16]). No interpolation or smoothing is used. In the present example, the TF coil diameter was $D = 1$ m, the major radius of its centre was $R = 0.6$ m and the angle of inclination $\gamma = 0.33$ rad, in accordance with the 'optimization rule' [16]:

$$\frac{DN \sin\gamma}{\pi R} \approx 1 \tag{1}$$

corresponding to the efficient generation of the $L = 1$ stellarator configuration, where L is the poloidal multipolarity. More generally, for different L, L should replace one in the right-hand side of (1), and D should stand for the vertical size of the coil.

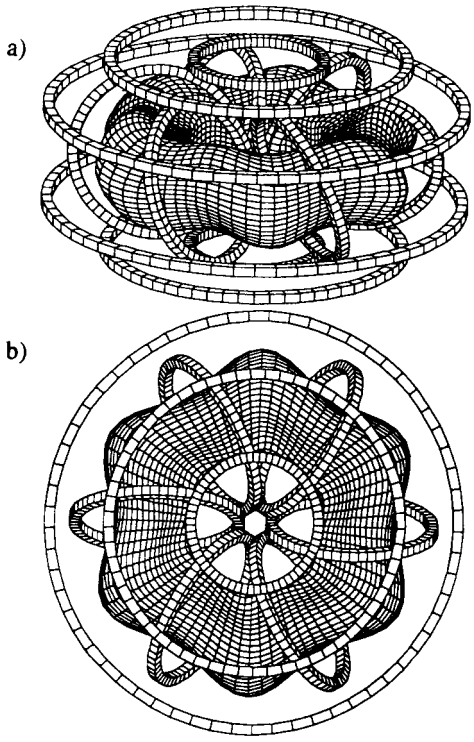

Figure 1. Side (a) and top (b) view of the LAR stellarator configuration with planar circular coils. The last closed flux surface is shown as well.

The top–bottom symmetric PF coil system has been chosen in accordance with the 'balance rule' and 'location rule', also formulated in [16]. The ratios of the currents in the PF rings to that in the TF coil were as follows: $I_1 = I_2 = 0.14$ (for the rings at $R = 1.25$ m and $R = 0.9$ m), and $I_3 = 0.6$ (for the rings at $R = 0.4$ m).

The main stellarator characteristics of the magnetic field are presented in figures 3(a, b). These are the rotational transform: $\iota = 1/q$, q being the safety factor; the magnetic well, $W(\rho) = 1 - V'(\Phi(\rho))/V'(0)$; where $V' = \mathrm{d}V/\mathrm{d}\Phi$ is the derivative of the enclosed volume over the enclosed toroidal magnetic flux, and the magnetic-field variation,

$$\eta = \frac{B_{\max} - B_{\min}}{B_{\max} + B_{\min}} \tag{2}$$

with $B_{\min}$ and $B_{\max}$ being the minimum and maximum values of the magnetic field at a given flux surface. In figure 3(a), the total rotational transform, ι, is shown together with its external ι_{ex}, and internal ι_{in}, components, calculated respectively for the outboard and inboard halves of flux surfaces [3]

$$\iota \approx \frac{2\iota_{\mathrm{ex}}\iota_{\mathrm{in}}}{\iota_{\mathrm{ex}} + \iota_{\mathrm{in}}}. \tag{3}$$

Projections of the coil system elements on the poloidal cross-section, together with cross sections of the last closed flux surface at toroidal angles $\varphi = 0$, $\pi/2N$, π/N, are shown in figure 4.

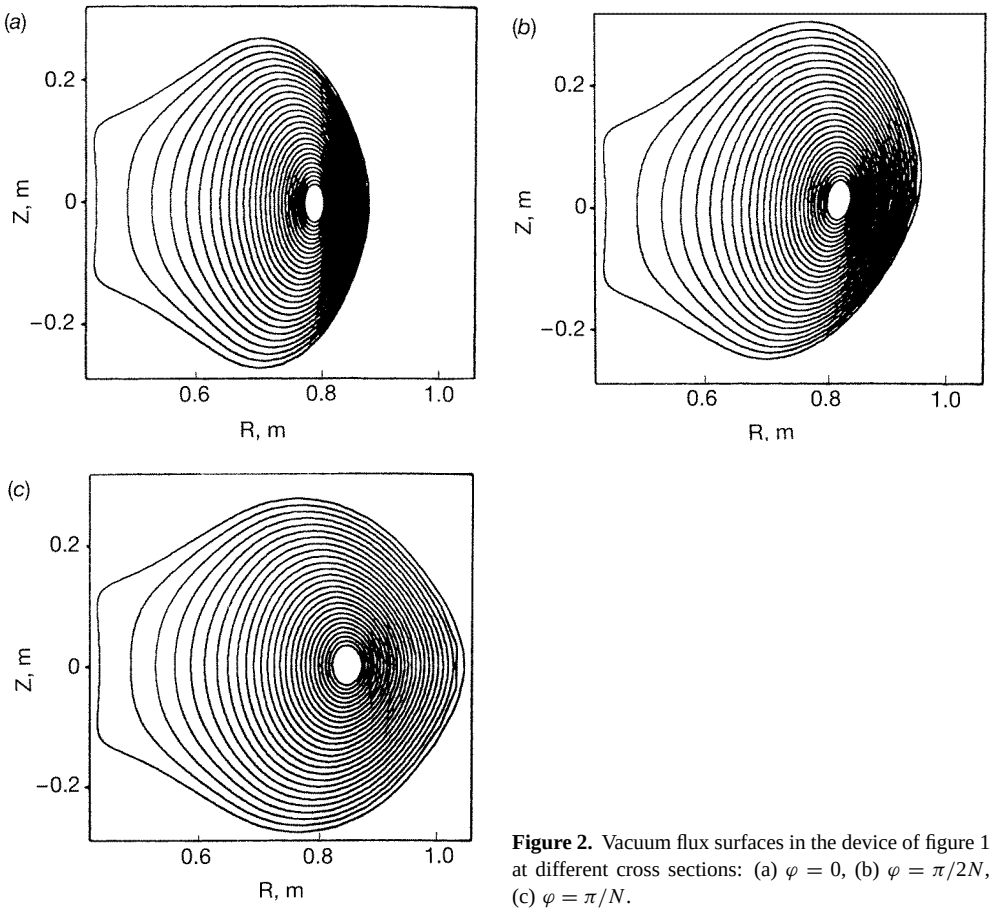

Figure 2. Vacuum flux surfaces in the device of figure 1 at different cross sections: (a) $\varphi = 0$, (b) $\varphi = \pi/2N$, (c) $\varphi = \pi/N$.

3. Bean-shaped flux surfaces

Bean-shaped plasmas are under investigation in tokamaks [19] and stellarators [9, 18, 20]. Usually this shape corresponds to the advanced high-β properties of the configuration. The bean-shaped plasmas can easily be formed in a SS by using an additional PF ring located in the equatorial plane at a small major radius. The planar inclined coils, however, can naturally produce bean-shaped plasmas without any additional current rings. One reason for that is clear, the internal (inboard) current filaments of the planar inclined coils produce an equivalent toroidal current.

This effect can be more profound if a TF coil is truncated, as shown in figure 5. The LARS device considered in this example has again six inclined TF coils and six PF rings. Circular TF coils of the same diameter as considered before are used, but because of truncation, the major radius of the coil centres is lower, $R = 0.4$ m. The side and the top views of this more compact configuration are presented in figures 6(a) and (b), while a set of corresponding closed flux surfaces is shown in figures 7(a)–(c). The rotational transform ι, the magnetic well W, and the magnetic-field variation η, are close to that found for LARS with circular coils (see figure 3) and thus do not require a separate figure. The configuration considered with the bean-shaped flux surfaces is more compact than the system with circular coils, and the aspect ratio is somewhat lower, $A \approx 1.8$.

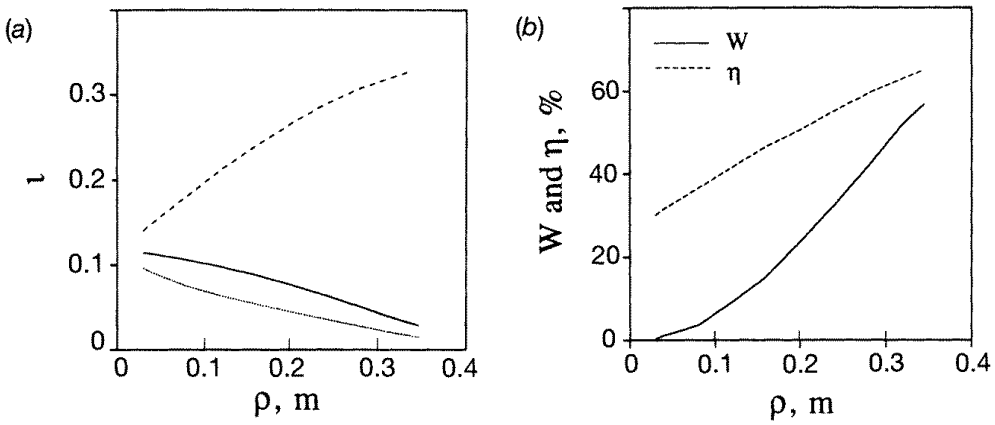

Figure 3. Radial dependence of a few parameters for the device of figure 1; (a) the total rotational transform (full curve) and its external (broken curve), and internal (dotted curve) components; (b) the magnetic well, W, and the magnetic-field variation, η.

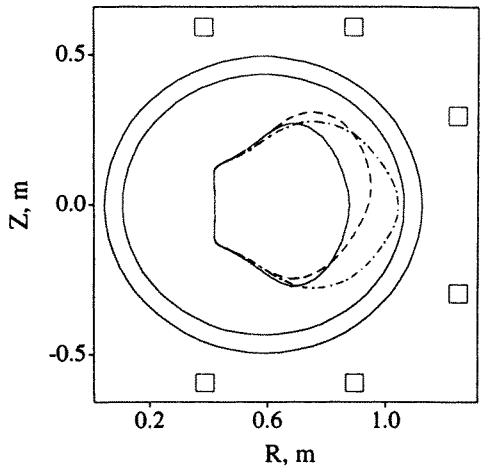

Figure 4. Poloidal cross section of the device of figure 1. Shown are the coil projections and the cross sections for the last closed flux surface at toroidal angles $\varphi = 0$ (full curve), $\pi/2N$ (broken curve), and π/N (chain curve).

In accordance with the optimization rule, (1), decreasing R requires decreasing the inclination angle γ. This configuration features, however, a rather low rotational transform, approximately a factor of two lower than that given in figure 3(a). To increase the rotational transform values back close to those given in figure 3(a), we chose a higher $\gamma \approx 0.6$ corresponding to the $L = 2$ configuration.

4. Coil system accommodating the central transformer

As was discussed in [3–6], the SS devices benefit from the plasma current: the rotational transform increases, higher β values can be reached, and the magnetic-field ripple can be

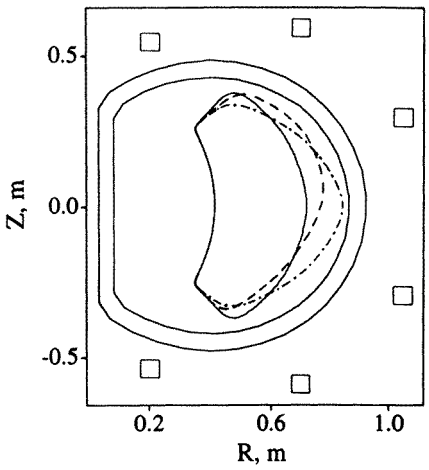

Figure 5. Same as figure 4, but for the device with truncated circular coils.

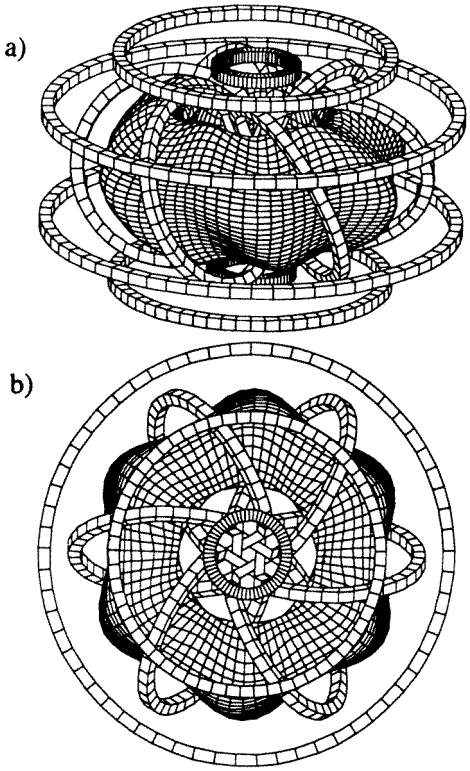

Figure 6. Side (a) and top (b) view of the device with truncated circular coils.

reduced substantially; also, as was stressed there, a SS can benefit not only from the ohmic current but from the bootstrap current as well, which flows in a SS in such a direction that its rotational transform enhances the vacuum rotational transform. The LARS considered with planar coils benefit from the plasma current in a similar way (section 6).

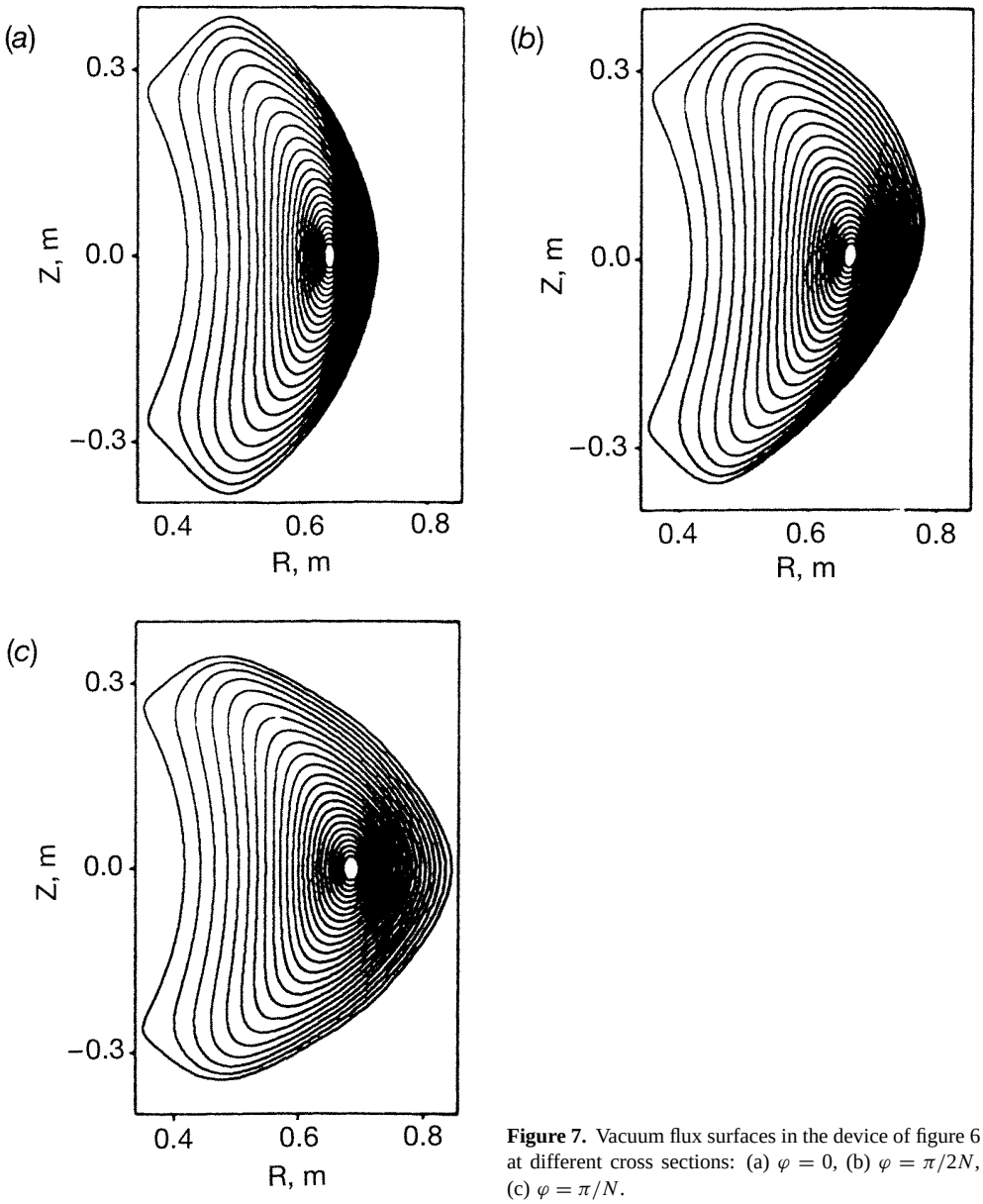

Figure 7. Vacuum flux surfaces in the device of figure 6 at different cross sections: (a) $\varphi = 0$, (b) $\varphi = \pi/2N$, (c) $\varphi = \pi/N$.

In a relatively small LARS one cannot rely on the strong bootstrap current. To enhance the capability of the configuration it is thus advantageous to have an ohmic current transformer. In principle the ohmic transformer windings can be formed around the inboard legs of the TF coils, similar to that in a Spherical Tokamak (ST). The ohmic transformer windings can also be located at some other place near the plasma [21], not necessarily at the small major radius. However, from an engineering point of view, it is often more convenient to have the ohmic transformer windings decoupled from the TF coils. Then there should be a space left for the central transformer, and the inboard legs of the TF coils have to be located at the larger major radius, as is done in a standard tokamak. This will

definitely cause an increase of the plasma aspect ratio; however, values of $A \approx 3$ can still be attained.

To obtain such a configuration, the TF inclined coils (such as, e.g., those considered in the two previous sections) can simply be moved further from the centre. This procedure, however, will increase the size of the device. Here we show a different way of accommodating the central transformer—adjusting the shape of the TF coils.

As an example, we consider a device similar to that with circular coils, presented in figure 1. The difference is in the following. The TF coils are slightly vertically elongated with elongation factor $\kappa = 1.2$, and inclined at the larger angle $\gamma \approx 0.6$, to increase the rotational transform, thus the $L = 2$ magnetic configuration is produced. The horizontal width of the TF coils (before modification) $D = 1$ m, and the major radius of their centres, $R_0 = 0.6$ m, are the same as before. The inboard parts of the TF coils are modified to go around the central transformer of radius $R_t = 0.3$ m. The projection of the TF coil obtained (together with the projections of the last closed flux surface cross-sections) are shown in figure 8, while the top view is given in figure 9. The set of closed flux surfaces is shown in figure 10. The main characteristics of the magnetic configuration, such as the rotational transform ι, the magnetic well W, and the magnetic field variation η, are presented in figures 11(a) and (b).

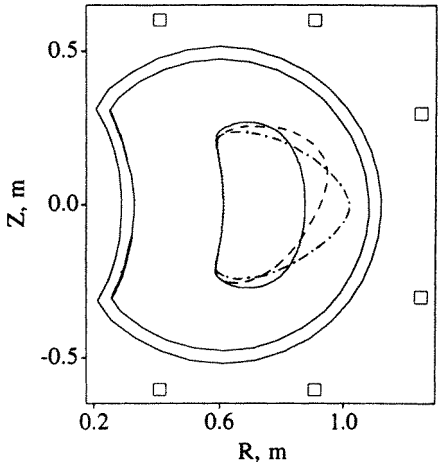

Figure 8. Same as figure 4, but for the device with the central transformer.

One can see that the obtained magnetic configuration features a rather high rotational transform, $\iota(0) = 0.2$ and its external component increases to $\iota_{ex} \approx 0.45$ at the last closed flux surface. The central location of the closed flux surfaces adds to the convenience of this configuration for fusion applications. The aspect ratio obtained, $A \approx 3.2$, however, is larger than in previous examples.

5. Internal set of flux surfaces and a natural divertor

As was mentioned in [16], inclined TF coils generally simultaneously produce two separate sets of closed flux surfaces: the internal one (at small major radii), and the external set (at larger major radii). The analysis of the properties of these two sets, as well as an explanation of the reasons for their existence, have also been presented in [16].

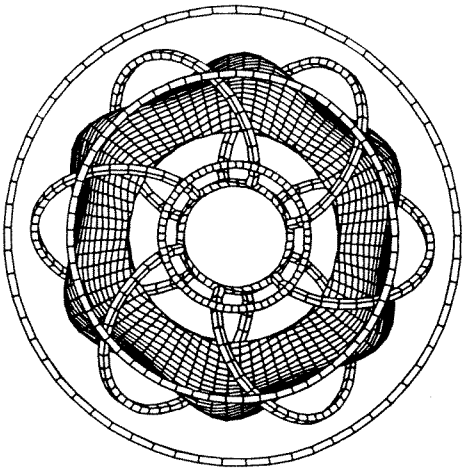

Figure 9. Top view of the device with the central transformer.

These two sets have opposite helicity, so the opposite helical harmonics are generated, and the magnetic-field lines rotate in opposite poloidal directions. These sets are very different at a low aspect ratio: the volume occupied by the internal set gradually decreases with decreasing A until it practically disappears at a very low A.

For the device considered in figures 8–11 with $A \approx 3.2$, the internal set still exists and the corresponding closed flux surfaces are presented in figures 12(a)–(c). The rotational transform for this set is $\iota(0) \approx -0.14$ at the magnetic axis and $\iota(1) \approx -0.09$ at the last closed flux surface shown.

The last closed flux surface in figure 12 shows some stochasticity. In principle, there are larger closed flux surfaces for an internal set. However, the stochasticity there is very strong, so it is reasonable to call it a stochastic region. The stochastic region can clearly be seen in figure 13 where the last flux surfaces from both sets are shown together. One can see that stochasticity is more profound for the edge of the internal set but is small for the external set.

At lower aspect ratios, the internal set of closed flux surfaces disappears. However, the natural divertor region caused by the residual of the internal set is still present. To demonstrate this, we again consider the set of flux surfaces of figure 4, for $A \approx 2.4$. The internal set is absent in this case, but the natural divertor region is present and is shown in figure 14 (the full curves show the closed flux surfaces while the broken ones indicate the opened field lines).

6. Effects of finite plasma pressure and plasma current

The advantages or disadvantages of any concept for controlled fusion have to be judged on the basis of its properties for the finite-pressure (finite-β) plasmas. In spite of the fact that initial experiments on any concept are usually carried out in rather small-scale devices with moderate plasma parameters, incapable of exploring the high-β behaviour, the future of the concept depends substantially on the capability to confine high-β plasmas.

The present paper describes a few novel and simple configurations with the planar coils. Leaving the full analysis of MHD equilibrium, stability, and transport in high-β plasmas

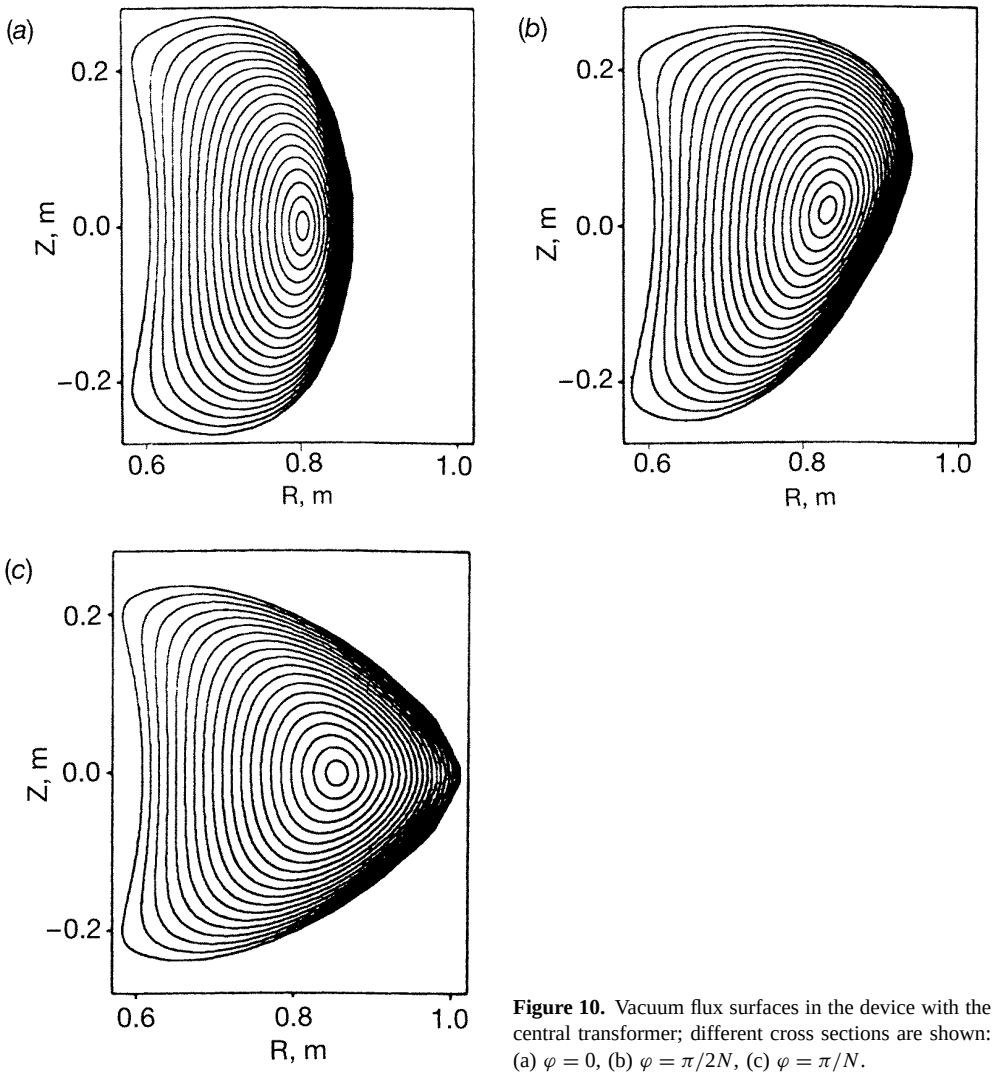

Figure 10. Vacuum flux surfaces in the device with the central transformer; different cross sections are shown: (a) $\varphi = 0$, (b) $\varphi = \pi/2N$, (c) $\varphi = \pi/N$.

in these devices for future research, we would still like to examine a few effects of the finite plasma pressure and finite plasma current. For these purposes we use the 3D MHD equilibrium code, VMEC [22], which is run in its free boundary mode. As an example, we present the results for the configuration of figure 1 with the circular inclined coils.

By increasing the plasma pressure, the shape of the plasma changes significantly and the magnetic axis shifts outboard (Shafranov shift). These effects might set the limit on the β values that can be reached in a device. In our calculations we suggest that the plasma pressure profile, $p \sim (1 - s)^2$, where $s = \Phi/\Phi_{\max}$ is the normalized enclosed toroidal magnetic flux. Figure 15 shows the three principal plasma cross sections for the finite-pressure plasma with the central β, $\beta_0 = 3\%$, and the volume average β, $\langle\beta\rangle = 1\%$. These values of β are close to the equilibrium limit for this configuration.

The limits on β can be increased significantly in the devices considered if there is a plasma current. This is probably a general feature of the LARS and has already been found for the SS configuration [5]. To demonstrate the positive effect of a small plasma

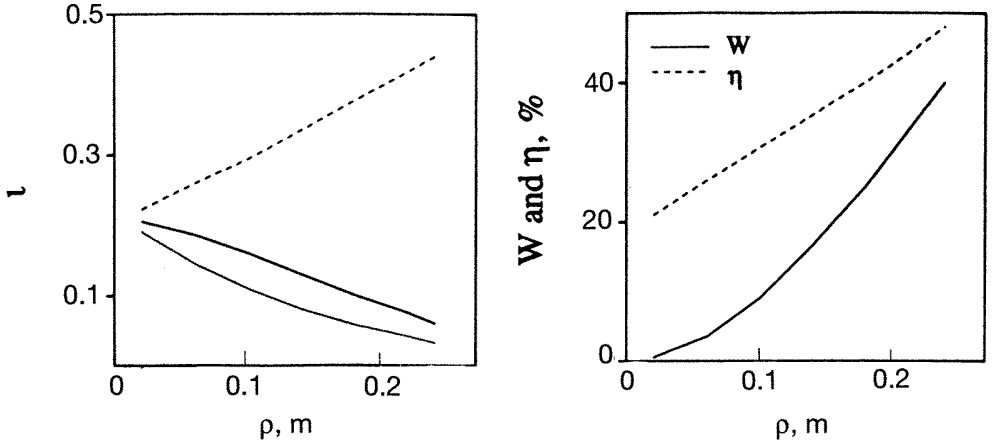

Figure 11. Same as figure 3 but for the device with the central transformer.

current we suggest that a toroidal current of $I_p = 28$ kA with a profile of $(1 - s)$ flows in the plasma. The results of calculations for $\beta_0 = 6\%$ and $\langle\beta\rangle = 2\%$ (this is not a limiting β) are presented in figures 16–18. Although the β values here are twice as high as in the previously considered currentless case, the plasma shape is closer to the vacuum configuration (figure 2). The total rotational transform (figure 17) is higher than that in the vacuum case (figure 3), because it also includes the contribution produced by the plasma current.

In principle the availability of the plasma current does not necessarily mean that this current has to be driven inductively, thus making a device a stellarator–tokamak hybrid. As was found in calculations for a large SS device [5, 6], for example, a strong bootstrap current can be the only source of the plasma current, thus making such a device a pure stellarator (with the plasma current, however).

7. Global scalings

As was discussed in [23], the neoclassical theory [24–28] predicts the following global energy-confinement time-scalings depending on the collisionality. For the so-called plateau regime of intermediate collisionality

$$\tau_E^{PL} \approx 0.35 a^2 R B^{0.8} n^{0.6} P^{-0.6} \iota^{0.4} \tag{4}$$

and for the low-collisional ripple-trapped-particle regime (usually, with a negative radial-electric field),

$$\tau_E^{RT} \approx 0.011 a^2 R^{1.22} B^{0.44} n P^{-0.78} \varepsilon_h^{-1/3} \tag{5}$$

where the energy confinement times τ_E^{PL} and τ_E^{RT}, are in seconds; the average minor plasma radius a, and the major radius R, are in meters; magnetic field strength B, in Tesla; average plasma density n, in 10^{19} m^{-3}; input power P, in MW; ι is the rotational transform at $\rho = 2/3$, and ε_h is the relative helical ripple at $\rho = 2/3$ corresponding to the simplified magnetic-field approximation

$$B/B_0 = 1 - \varepsilon_t \cos\theta - \varepsilon_h \cos\eta \tag{6}$$

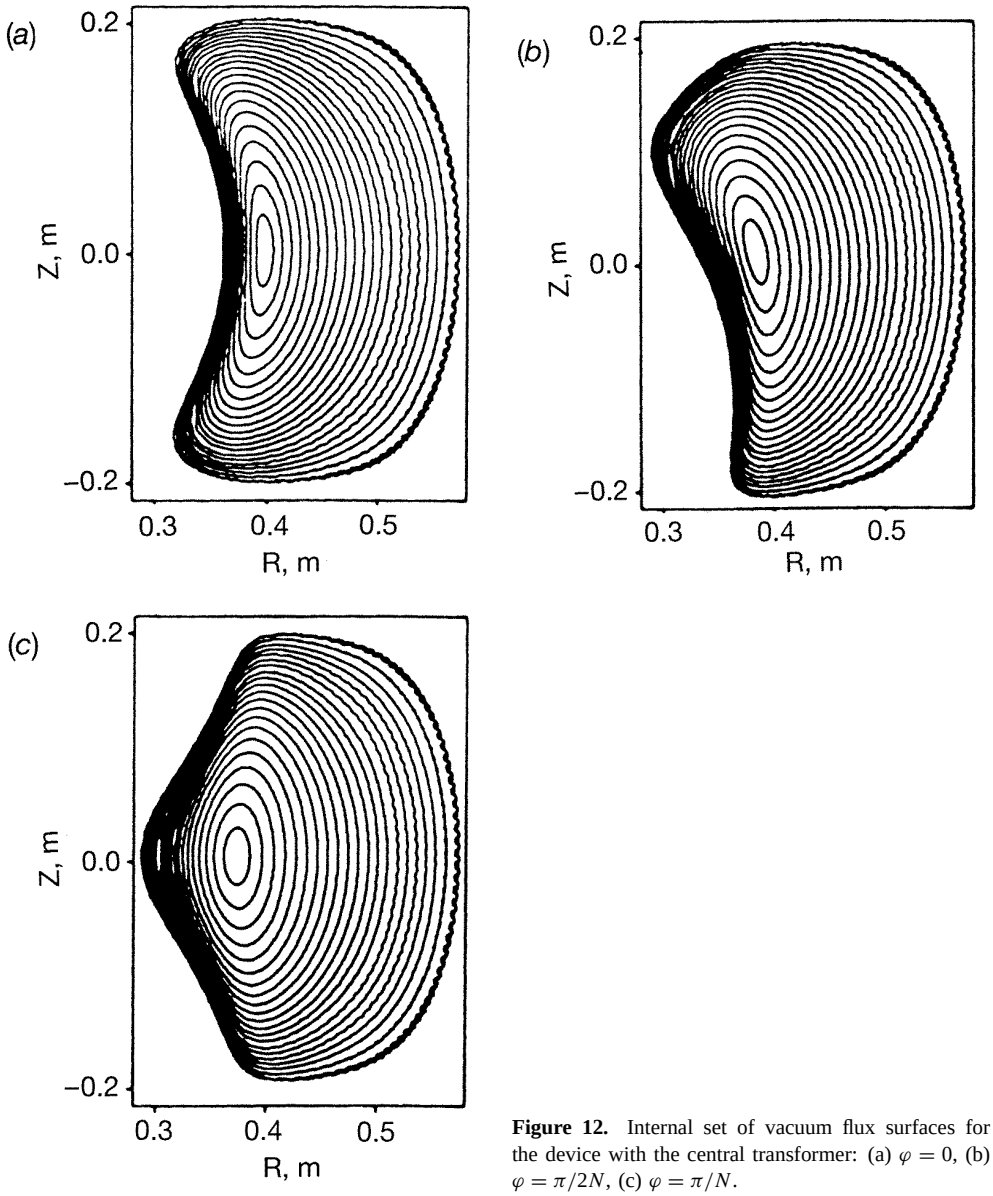

Figure 12. Internal set of vacuum flux surfaces for the device with the central transformer: (a) $\varphi = 0$, (b) $\varphi = \pi/2N$, (c) $\varphi = \pi/N$.

with B_0 being the central magnetic field, $\eta = m\theta - nN\varphi$, m and n are the poloidal and toroidal mode numbers, N is the number of toroidal field periods, and θ and φ are the poloidal and toroidal angles.

However, the experimentally obtained energy-confinement times in stellarators are usually shorter than those given above, which stresses that the 'anomalous' energy transport, usually attributed to mode activity and turbulence, is of significant importance in stellarators.

The comprehensive analysis of the experimental data for the major known stellarator devices has resulted in a few experimental scalings. In spite of the fact that the stellarators taken into consideration had very different geometrical and physical properties (different size, aspect ratio, rotational transform, magnetic-field strength, helical ripple, etc), it was

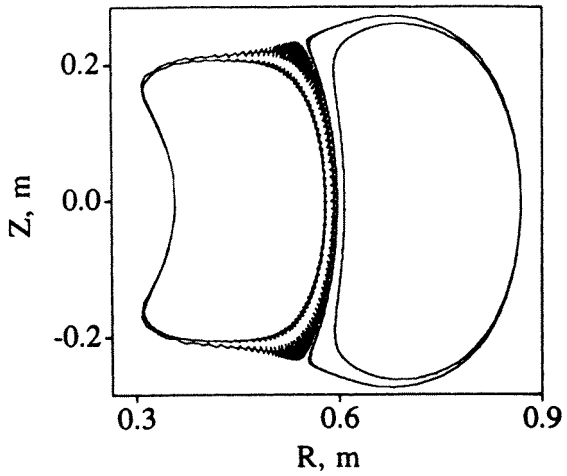

Figure 13. Stochastic region between the two sets of closed flux surfaces for the device with the central transformer.

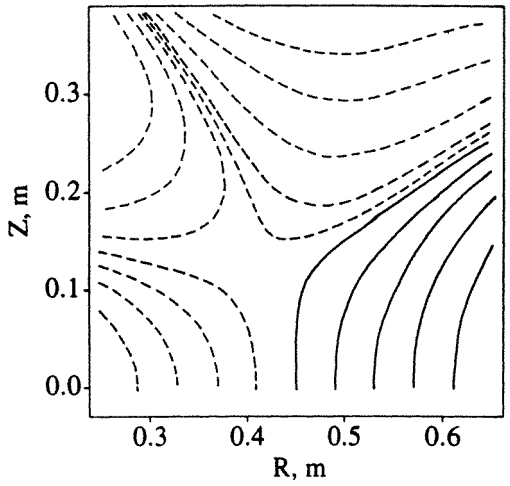

Figure 14. Field line traces demonstrating the divertor configuration. Full curves correspond to the closed flux surfaces, broken curves show the opened field lines.

possible to combine the results from all the machines into the single scalings. The most well known and widely used scalings for stellarators are the following. These are the so-called LHD scaling [23],

$$\tau_{\mathrm{E}}^{\mathrm{LHD}} = 0.035 a^2 R^{0.75} B^{0.84} n^{0.69} P^{-0.58} \tag{7}$$

the International Stellarator Scaling 1995 (ISS95) [29],

$$\tau_{\mathrm{E}}^{\mathrm{ISS95}} = 0.079 a^{2.21} R^{0.65} B^{0.83} n^{0.51} P^{-0.59} \iota^{0.4} \tag{8}$$

and the Lackner–Gottardi (LG) scaling [30] which can be re-written [29] in stellarator notations as

$$\tau_{\mathrm{E}}^{\mathrm{LG}} = 0.043 a^2 R B^{0.8} n^{0.6} P^{-0.6} \iota^{0.4}. \tag{9}$$

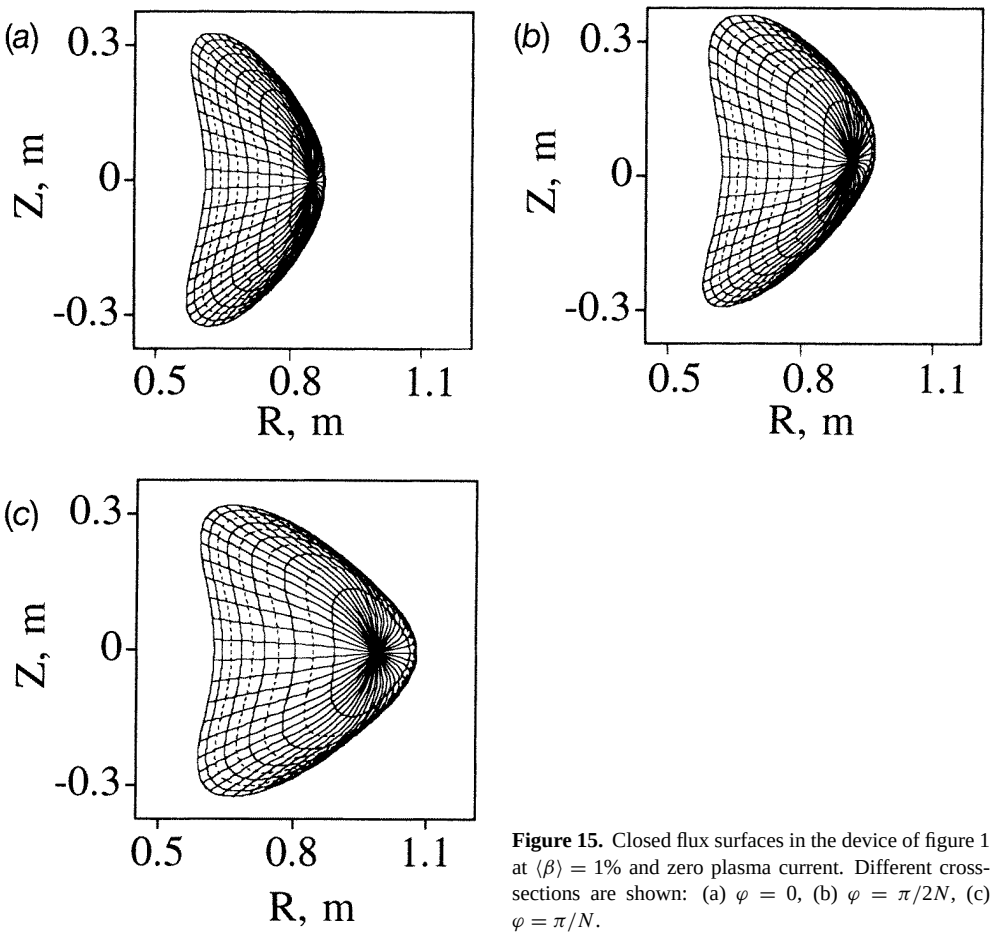

Figure 15. Closed flux surfaces in the device of figure 1 at $\langle\beta\rangle = 1\%$ and zero plasma current. Different cross-sections are shown: (a) $\varphi = 0$, (b) $\varphi = \pi/2N$, (c) $\varphi = \pi/N$.

One can see that the LG scaling differs from the plateau regime scaling (4), by the coefficient only and gives τ_E values which are about eight times shorter.

All the above experimental scalings, (7)–(9), give a fairly good description of standard experimental data not only for stellarators (enhanced regimes such as H-mode are excluded) but also for tokamaks (L-mode regimes). It is also interesting to note that in spite of the fact that the iota-independent LHD scaling was originally based on the experimental data from stellarators Heliotron-E, W7-A, L2 and Heliotron DR, it also gives the best description of experimental data for other stellarators considered in [29], such as W7-AS, ATF and CHS. The ISS95 scaling, however, is probably the best for approximation of the whole set of experimental data from both the stellarators and tokamaks.

Two more important experimental scalings for stellarators have been discussed in [23]. Those are for the critical plasma density,

$$n_c = \min\{2.5(PB/a^2R)^{0.5}, 3.5PB^{0.5}/aR\} \tag{10}$$

and for the critical triple product, $nT\tau_E$, which can be reached in the device,

$$nT\tau_E = 0.045a^{0.6}R^{-0.2}B^{2.4}P^{0.54} \tag{11}$$

where T is the plasma temperature in keV. The expression (11), shows clearly that, in principle, the low aspect ratio and high magnetic field are the most important factors of the

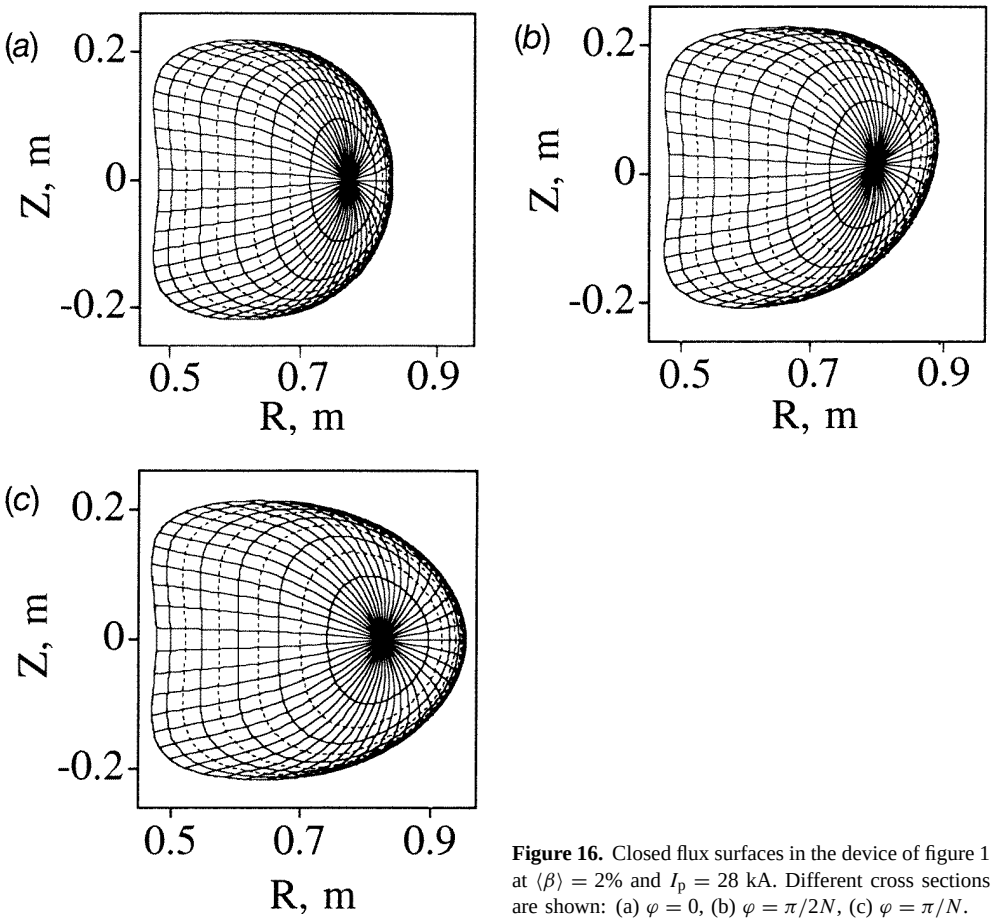

Figure 16. Closed flux surfaces in the device of figure 1 at $\langle\beta\rangle = 2\%$ and $I_p = 28$ kA. Different cross sections are shown: (a) $\varphi = 0$, (b) $\varphi = \pi/2N$, (c) $\varphi = \pi/N$.

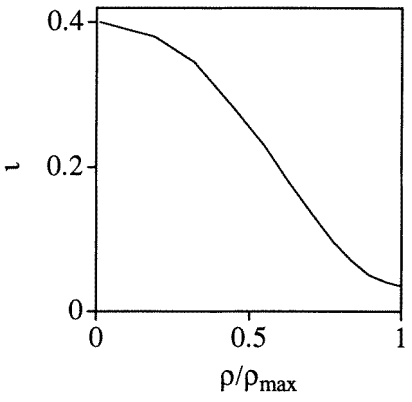

Figure 17. Radial dependence of the total rotational transform for the equilibrium of figure 16.

device which are favourable for controlled fusion, aside from the problem of the possible loss of high-energy particles (such as alpha-particles) in the case of non-optimized configurations.

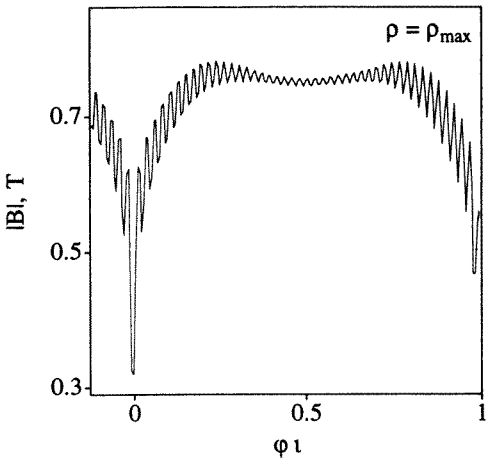

Figure 18. Magnetic-field variation along a field line for the equilibrium of figure 16 (edge flux surface).

Let us consider an example of the LARS configuration of figure 16 produced by planar circular coils. It has $a \approx 0.2$ m, $R \approx 0.7$ m, $B \approx 0.65$ T (for the currents in TF coils of 300 kA), $\iota \approx 0.2$ and $\varepsilon_h \approx 0.1$. Suggesting the input power of $P = 0.5$ MW, equation (10) gives $n_c \approx 10^{20}$ m^{-3}, which is a rather high value. Taking a more moderate number for the average plasma density, $n = 5 \times 10^{19}$ m^{-3}, one reaches the following values for the energy confinement times:

$$\tau_E^{PL} \approx 15 \text{ ms} \qquad \tau_E^{RT} \approx 4.4 \text{ ms} \qquad \tau_E^{LHD} \approx \tau_E^{ISS95} \approx 3 \text{ ms} \qquad \tau_E^{LG} \approx 2 \text{ ms}. \tag{12}$$

The neoclassical energy-confinement times (even in the case of low collisionality) are larger than that given by the experimental scalings and thus not of primary importance for the device with the parameters considered. However, scaling the geometrical size, the plasma density and the magnetic field by a factor C, and the input power by C^3 (proportional to the volume), one can find that the neoclassical ripple-induced confinement time τ_E^{RT}, grows as $C^{2.3}$, which is somewhat slower than the growth of the experimental scaling times proportional to $C^{2.45} - C^{2.6}$. This will make the neoclassical ripple-induced transport of thermal particles of importance for significantly larger machines of this type.

For energetic particles (such as alpha particles in a reactor, or energetic particles induced by the neutral beam injection or powerful minority ICRF heating), even in a device of moderate size, the confinement depends mostly on the outboard magnetic-field ripple, which hence should be reduced. One possible way of reducing such a ripple in considered LARS configurations with planar coils might be the addition of a significant amount of the plasma current.

The discussed LARS configurations (except the internal set, considered in section 5 and shown in figure 12) feature an unfavourable location for the magnetic-field ripple. For illustration, the $|B|$-variation along the field line for the equilibrium of figure 16 (the edge flux surface is considered, where the variation of $|B|$ is the strongest) is shown in figure 18. Significant optimization of the configuration regarding the particle and energy losses can be obtained [31, 32], for example, by a modification of the coils in such a way that the location of the magnetic ripple is moved from the outboard to the inboard of the toroidal plasma. Such optimization, however, might result in the non-planar coils, and is outside the scope of the present paper. The internal set produced by the planar inclined coils, however, is already optimized in this regard.

8. Discussion and conclusions

The LARS configurations produced by the planar inclined coils were investigated. The aspect ratios A of such configurations are somewhat larger than in the concept of a Spherical Stellarator proposed and analysed in [3–6]. However, there is the advantage of planar coil simplicity.

Different types of possible configurations with planar coils, having attractive parameters such as a large enclosed volume, significant external rotational transform, and strong magnetic well, were identified. The advantage of a natural toroidally symmetrical divertor region, existing in the configurations with the planar inclined coils, was demonstrated as well. The divertor region, in the low-A configurations considered with the inclined coils, appears as a residual of the internal set of closed flux surfaces, which is normally present at larger aspect ratios [16].

Examples include very simple and inexpensive devices, such as devices with circular coils, with truncated circular coils, and with the planar coils accommodating the central ohmic transformer. It was shown that plasmas of different shapes, including the bean shape, can be produced naturally in such systems.

One of the main new ideas behind the Spherical Stellarator concept [3–6] is that the plasma current is an important factor for improving many characteristics of such devices. In this paper it has been shown that LARS devices with planar coils benefit from the plasma current as well.

Plasma energy and particle losses are very important characteristics of a device, and the corresponding analysis has to be carried out for a full assessment of any concept proposed for controlled fusion research. The present paper includes just a preliminary analysis based on the global scalings which show that the considered LARS devices with planar coils, at moderate parameters, can confine the plasma fairly well. The projection to the larger devices with the reactor parameters, however, is not optimistic for the external sets of flux surfaces which feature the outboard location of the magnetic-field ripple. The internal set considered in section 5, however, is already optimized (according to [31, 32]) for the transport, and thus can represent an interesting case for further investigation.

In conclusion, the low aspect ratio and strong magnetic field are the main factors (aside from the problem of the possible loss of high-energy particles) favourable for reaching the advanced plasma parameters. The initial analysis of LARS with planar coils shows that planar coils offer the possibility of a configuration with rather attractive properties such as: coil compactness and simplicity (which means low cost of manufacture and device construction and the high accuracy of the assembly), large enclosed volume, relatively large external rotational transform, natural and simple toroidally symmetric divertor or even two sets of closed flux surfaces. The internal set of flux surfaces has optimized characteristics for particle confinement. Further analysis and optimization is necessary for a more complete assessment of this LARS approach.

Acknowledgments

The author would like to acknowledge useful discussions with D B Batchelor, E F Jaeger, B A Carreras, S P Hirshman, D A Spong, A J Wootton, R Gandy, J D Hanson, S F Knowlton and J D Callen. This research was supported by the US DoE grant No DE-FG02-97ER54395.

References

[1] Hawryluk R J and TFTR Team 1995 Review of recent D-T experiments from TFTR *Proc. 15th IAEA Conf. Plasma Phys. and Contr. Nucl. Fus. Res. (Seville, 1994)* vol 1 (Vienna: IAEA) p 11

[2] Rebut P-H, Chuyanov V, Huguet M, Parker R R, Shimomura Y and the ITER Joint Central Team and Home Teams 1995 The ITER EDA outline design *Proc. 15th IAEA Conf. Plasma Phys. and Contr. Nucl. Fus. Res., (Seville, 1994)* vol 2 (Vienna: IAEA) p 451

[3] Moroz P E 1996 Spherical stellarator configuration *Phys. Rev. Lett.* **77** 651

[4] Moroz P E 1996 Spherical stellarator approach *23rd IEEE Conf. Plasma Science (Boston, MA)* (Piscataway, NJ: IEEE) p 190

[5] Moroz P E 1996 Spherical stellarator with plasma current *Phys. Plasmas* **3** 3055

[6] Moroz P E, Batchelor D B, Carreras B A, Hirshman S P, Lynch V E, Spong D A, Tolliver J S, Ware A S and Whitson J C 1996 Ultra low aspect ratio stellarator or hybrid configurations *Fusion Technol.* **30** 1347

[7] Nishimura K *et al* 1990 *Fusion Technol.* **17** 86

[8] Knowlton S F, Gandy R F, Hanson J D, Hartwell G J and Lin H 1993 *J. Fusion Energy* **12** 261

[9] Blackwell B D *et al* 1995 *Proc. 15th IAEA Int. Conf. on Plasma Phys. and Contr. Nucl. Fusion Res. (Seville, 1994)* vol 2 (Vienna: IAEA) p 337

[10] Popov S N and Popryaduhin A P 1966 *Sov. Phys.–Tech. Phys.* **11** 284

[11] Ivanovsky M A, Popov S N and Popryaduhin A P 1973 *Stellarators* vol 65, ed D B Skobel'tsin (Moscow: Nauka) p 65 (in Russian)

[12] Reiman A and Boozer A 1983 *Phys. Fluids* **26** 3167

[13] Georgievskij A V, Ziser V E, Nemov V V, Peletminskaya V G, Pogozhev D P, Sergeev Yu F, Skoblik M N and Shishkin A A 1974 *Nucl. Fusion* **14** 79

[14] Bykov V E *et al* 1989 *Proc. 12th IAEA Int. Conf. Plasma Phys. Contr. Nucl. Fus. Res. (Nice 1988)* vol 2 (Vienna: IAEA) p 403

[15] Georgievskij A V, Martynov S A, Rudakov V A, Sergeev Yu A and Khodyachikh V A 1989 *Vopr. Atomn. Nauki i Tekh., Ser.: Termoyad. Sintez* **4** 28 (in Russian)

[16] Moroz P E 1995 Vacuum flux surfaces produced by the inclined coils *Phys. Plasmas* **2** 4269

[17] Sykes A *et al* 1995 *Proc. 15th Int. Conf. Plasma Phys. Contr. Fus. Res. (Seville, 1994)* vol 1 (Vienna: IAEA) p 719

[18] Alejaldre C *et al* 1990 *Fusion Technol.* **17** 131

[19] Bell R E *et al* 1990 *Phys. Fluids* B **2** 1271

[20] Beidler C *et al* 1990 *Fusion Technol.* **17** 148

[21] Buttery R, Counsell G, Cox M, Hender T C, Knight P J, O'Brien M R, Robinson D C, Voss G M and Wilson H R 1995 *Proc. 15th IAEA Conf. Plasma Phys. Contr. Nucl. Fus. Res. (Seville, 1994)* vol 2 (Vienna: IAEA) p 633

[22] Hirshman S P, Van Rij W I and Merkel P 1986 *Comput. Phys. Commun.* **43** 143

[23] Sudo S, Takeiri Y, Zushi H, Sano F, Itoh K, Kondo K and Iiyoshi A 1990 *Nucl. Fusion* **30** 11

[24] Galeev A A, Sagdeev R Z, Furth H P and Rosenbluth M N 1959 *Phys. Rev. Lett.* **22** 511

[25] Connor J W and Hastie R J 1974 *Phys. Fluids* **17** 114

[26] Hirshman S P and Sigmar D J 1981 *Nucl. Fusion* **21** 1079

[27] Kovrizhnykh L M 1984 *Nucl. Fusion* **24** 851

[28] Ho D D-M and Kulsrud R M 1987 *Phys. Fluids* **30** 442

[29] Stroth U, Murakami M, Dory R A, Yamada H, Okamura S, Sano F and Obiki T 1996 *Nucl. Fusion* **36** 1063

[30] Lackner K and Gottardi N A O 1990 *Nucl. Fusion* **30** 767

[31] Mynick H E, Chu T K and Boozer A H 1982 *Phys. Rev. Lett.* **48** 322

[32] Shaing K C and Hokin S A 1983 *Phys. Fluids* **26** 2136